JACS
JOURNAL OF THE AMERICAN CHEMICAL SOCIETY
Article
pubs.acs.org/JACS

Supramolecular Buffering by Ring−Chain Competition

Tim F. E. Paffen,[†,‡] Gianfranco Ercolani,[∥] Tom F. A. de Greef,*[,†,§] and E. W. Meijer*[,†,‡]

[†]Institute for Complex Molecular Systems, [‡]Laboratory of Macromolecular and Organic Chemistry, and [§]Computational Biology, Eindhoven University of Technology, P.O. Box 513, 5600 MB Eindhoven, The Netherlands

[∥]Dipartimento di Scienze e Tecnologie Chimiche, Università di Roma Tor Vergata, Via della Ricerca Scientifica, 00133 Roma, Italy

Supporting Information

ABSTRACT: Recently, we reported an organocatalytic system in which buffering of the molecular catalyst by supramolecular interactions results in a robust system displaying concentration-independent catalytic activity. Here, we demonstrate the design principles of the supramolecular buffering by ring−chain competition using a combined experimental and theoretical approach. Our analysis shows that supramolecular buffering of a molecule is caused by its participation as a chain stopper in supramolecular ring−chain equilibria, and we reveal here the influence of various thermodynamic parameters. Model predictions based on independently measured equilibrium constants corroborate experimental data of several molecular systems in which buffering occurs via competition between cyclization, growth of linear chains, and end-capping by the chain-stopper. Our analysis reveals that the effective molarity is the critical parameter in optimizing the broadness of the concentration regime in which supramolecular ring−chain buffering occurs as well as the maximum concentration of the buffered molecule. To conclude, a side-by-side comparison of supramolecular ring−chain buffering, pH buffering, and molecular titration is presented.

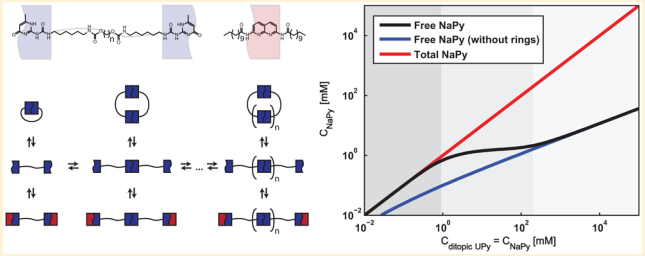

1. INTRODUCTION

Recent advances in functional molecular systems focus on increasing the number of components to, for example, design "smart" materials that can integrate multiple inputs.[1] This increase correlates with a transition in chemistry which is expanding from the synthesis of individual molecules to the construction of chemical networks that are better equipped to adapt to a multitude of environmental cues.[2] To match the level of complexity and responsiveness of biochemical pathways, artificial chemical networks should be composed of tens of different types of molecules each with its own well-designed function.[3] However, while individual molecules are at a point where their interactions can be rationally designed, only recently chemists have started to design large molecular networks of interacting molecules.[4]

Using a top-down approach, systems biologists are working to deduce the underlying mechanisms of a variety of cellular functions, while chemists are expanding their knowledge on molecular systems using a bottom-up approach.[5] Recent advances in the field of systems chemistry include, but are not limited to molecular recognition using dynamic molecular networks,[4e,6] self-replicating molecules by templating,[7] self-replicating aggregates,[8] and the construction of logic gates using self-replicators.[9] These fascinating advances are paving the way to systematically recreate specific cellular functions and to obtain a molecular-level understanding of the design principles governing those functions.

Buffering is a well-known term in chemistry, and the concept is used in a multitude of varying applications such as biochemical synthesis and assays, organic synthesis,[10a] fermentation processes,[10b] and dye processing.[10c] However, it is striking that, in chemistry, the scope of the buffered molecule is limited mainly to protons. Indeed, the very definition of a buffer, within a chemical context, is "any solution that maintains an approximately constant pH despite small additions of acid or base."[11] Contrastingly, in natural systems, the scope of buffering is much broader as biomolecular pathways employ regulation of component concentrations so that important processes become robust to concentration fluctuations. In those pathways, regulation is achieved by various mechanisms such as active negative feedback loops, passive autoinhibition effects, or molecular titration.[12] These regulatory mechanisms can display similar behavior as compared to "classical" pH buffers. For example, molecular titration in gene regulatory circuits leads to ultrasensitive thresholds at the equivalence point which is similar to the sharp increase in pH at the equivalence point of a titration curve. However, a challenge remains for chemists to broaden their definition of buffering and to recreate component regulation in synthetic systems.

Component buffering has also been observed in supramolecular systems as exemplified by the buffering of amphiphilic molecules that can form micelles (critical micelle concentration) and buffering in cooperative supramolecular polymerizations where the free monomer concentration becomes independent of the total concentration at high concentrations.[13] However, to date, there have been no applications that employ the molecular buffering observed in

Received: October 27, 2014
Published: January 12, 2015

DOI: 10.1021/ja5110377
J. Am. Chem. Soc. 2015, 137, 1501−1509

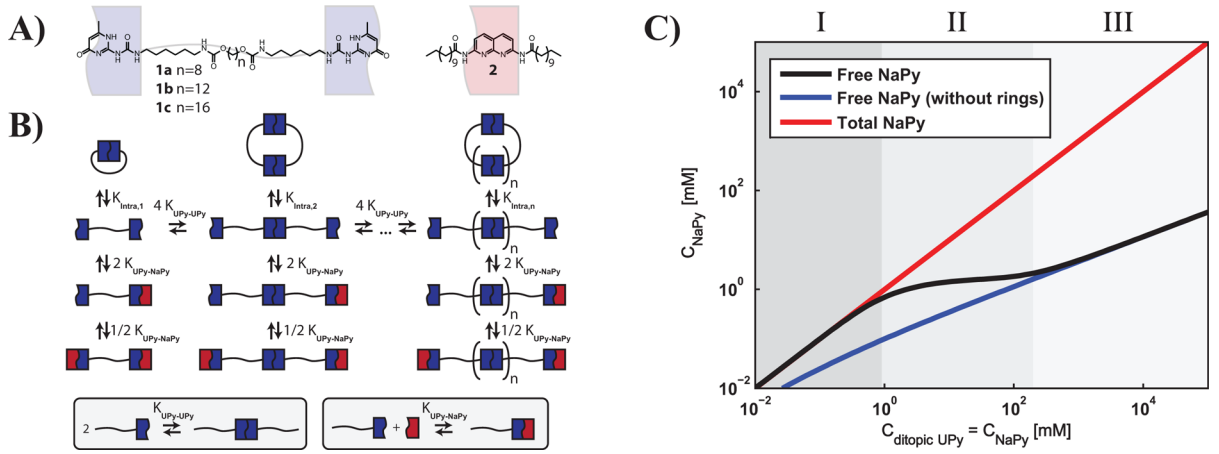

Figure 1. (A) Molecular structures of ditopic UPys **1a**–**c** and NaPy **2**. (B) Schematic overview of the supramolecular ring–chain buffering system with corresponding equilibrium constants. The employed statistical factors are a result of molecular symmetry and are directly related to the number of ways in which both reactants and products can be formed. (C) Predicted buffering of free NaPy based on the thermodynamic model for equimolar mixtures of ditopic UPy and NaPy ($K_{UPy-UPy}$ = 6 × 10^7 M^{-1}, $K_{UPy-NaPy}$ = 5 × 10^6 M^{-1}, EM = 100 mM, and f = 1).

these types of systems due to the inherent difficulties in designing a monomer that performs a function in its monomeric form but cannot perform the same function in the aggregated state, although examples exist where a function is performed only by the aggregated state or where only the monomer, and not the aggregate, is racemizable.[14] However, in these systems, component buffering was not investigated. Furthermore, designing component buffering in cooperative supramolecular polymerizations is not straightforward because it requires a high degree of control over both the nucleation and elongation phase.

Recently, our group reported on a system of two molecules that showed supramolecular buffering of one of the components.[15] The system consists of ditopic 2-ureido-pyrimidinone (UPy) molecule **1**, which can form both rings and chains, combined with monotopic 2,7-diamido-1,8-naphthyridine (NaPy) molecule **2** that acts as a chain stopper (Figure 1a). It was found that NaPy **2** acts as an organocatalyst in the Michael reaction of *trans*-β-nitrostyrene and 2,4-pentanedione. Subsequent investigations have shown that the catalytic activity of NaPy **2** is more complex than previously reported and that it most probably acts as a buffered phase transfer catalyst.[16] Here, we focus on the observation that the concentration of free NaPy ($C_{NaPy-free}$) can be buffered over a large concentration range when the concentrations of both NaPy ($C_{NaPy-total}$) and ditopic UPy ($C_{ditopic\ UPy}$) are increased simultaneously in a 1:1 ratio. The molecular mechanism by which component buffering occurs is described by a two-component equilibrium model that describes competition between cyclization and chain growth of a ditopic molecule and end-capping by a monotopic component. Furthermore, we show that supramolecular ring–chain buffering is not just limited to the system of ditopic UPy **1** and NaPy **2**, but that this concept can be applied using various noncovalent binding groups, as long as the molecular topology and binding constants are designed correctly.

2. RESULTS AND DISCUSSION

2.1. Model Outline. To gain a more intuitive understanding of the supramolecular ring–chain buffering, a thermodynamic equilibrium model is constructed. The basis for the model is the Jacobson–Stockmayer theory describing ring–chain equilibria of ditopic molecules.[17] A key parameter in this model is the effective molarity, which is the experimentally measured tendency of ring formation of a chain consisting of i ditopic molecules (EM_i). The EM is equivalent to the concept of effective concentration, which is the theoretical local concentration of associating groups around the ends of an end-tethered ditopic molecule assuming the linker follows Gaussian chain statistics.[18] In such a case, only strainless cycles are formed and the EM and the number of ditopic residues in a chain, i, are related in the following way:

$$EM_i = Bi^{-5/2} \quad (1)$$

where B is equal to the effective molarity of the strainless monomeric ring. The term $i^{-5/2}$ may be regarded as the product of $i^{-3/2}$ and i^{-1}, where the former relates to the probability that a Gaussian chain of i repeating units has its ends coincide and the latter to the number of equivalent bonds available for the ring-opening of a cyclic i-mer.

The Jacobson–Stockmayer model was later expanded to include finite intermolecular equilibrium constants (K_{inter}) and a description of the cycle distribution under dilute conditions.[19] In applying the theory to describe experimental systems, the assumption of strainless rings is not always met. Most often this is the case when the amount of linker atoms between the associating groups is less than 30 and monomeric rings are strained.[20] In such a case, it is still possible to describe the distribution of rings and chains provided that the EM values of the strained rings are known. The EM values of the strainless rings can then be computed using eq 1 in which B corresponds to the effective molarity that the monomeric ring would have if it were strainless.[19]

In the two-component model of supramolecular ring–chain buffering, end-capping reactions of chains are incorporated (Figure 1b; see the Supporting Information (SI) for full model details). The input parameters of the model are the UPy–UPy and UPy–NaPy binding equilibrium constants ($K_{UPy-UPy}$ and $K_{UPy-NaPy}$, respectively), the effective molarity of the monomeric ring (EM_1), and the ratio of NaPy to ditopic UPy (f). Gratifyingly, using the model to calculate the free NaPy concentration ($C_{NaPy-free}$) for various total concentrations of equimolar mixtures of ditopic UPy ($C_{dt-UPy-total}$) and NaPy ($C_{NaPy-total}$), a buffering plateau is observed (Figure 1c, region

DOI: 10.1021/ja5110377
J. Am. Chem. Soc. 2015, 137, 1501–1509

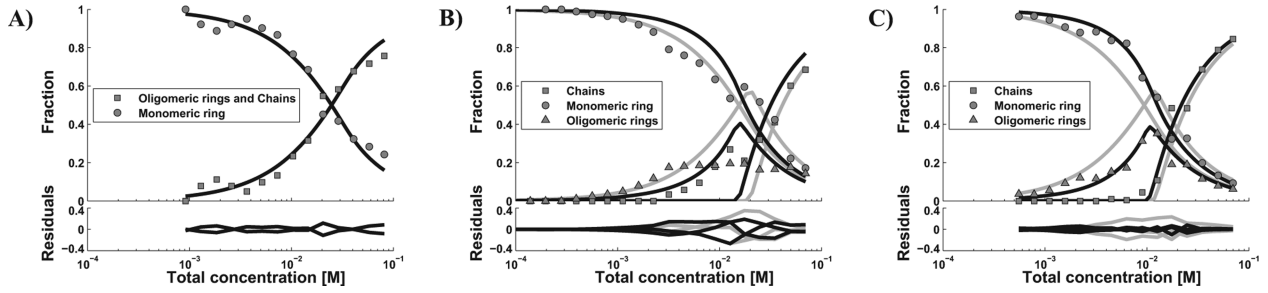

Figure 2. Speciation plot of ^{1}H NMR data (markers) of ditopic UPys **1a** (A), **1b** (B), and **1c** (C) and fits (lines) based on the thermodynamic ring−chain model using 1 (gray) and 2 (black) EMs. Residuals of both fits are shown.

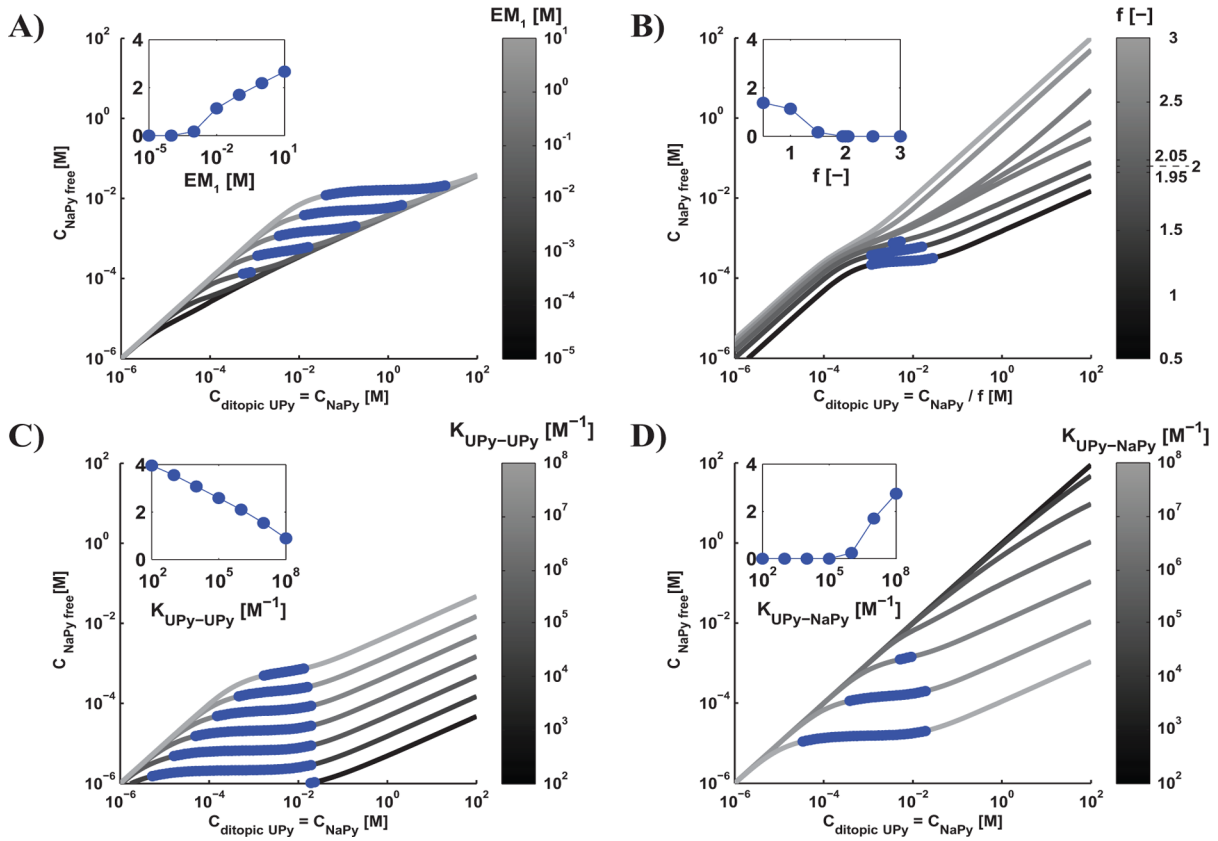

Figure 3. Predicted free NaPy concentration versus total concentration using different values for (A) EM_1, (B) f, (C) $K_{UPy-UPy}$, and (D) $K_{UPy-NaPy}$. The exact values used are shown next to the corresponding color bar. Note that in plot B the values used for f are not monotonically increasing to demonstrate the sensitivity of the buffering at values of f close to 2. The round marks superimposed on the curves denote the buffering plateau defined as the region where the moving three point average of $C_{NaPy\text{-}free}$ varies less than 10%. Insets show the corresponding broadness of the plateau (in decades) versus the parameter that is varied. If parameters are not varied, the following values are used: $K_{UPy-UPy} = 6 \times 10^7$ M^{-1}, $K_{UPy-NaPy} = 5 \times 10^6$ M^{-1}, $EM_1 = 10$ mM, and $f = 1$.

II). Based on these simulations, three distinct concentration regions are observed. At low concentrations, $C_{NaPy\text{-}free}$ is equal to $C_{NaPy\text{-}total}$ and the system consists of free NaPy and ditopic UPy rings (I). Upon increasing concentrations of both components, the buffering region is observed, where $C_{NaPy\text{-}free}$ is almost constant (II). As the fraction of bound NaPy starts to increase, the composition of the system becomes a mixture of both rings and end-capped chains. At the highest concentrations, $C_{NaPy\text{-}free}$ increases linearly again and the system comprises mainly end-capped chains (III). Indeed, in region III, the $C_{NaPy\text{-}free}$ curves of both the systems with and without rings overlap (black and blue lines, respectively).

Interestingly, the transition from region II to III is equal to the critical concentration (C_{cr}), at which point any subsequent addition of ditopic molecules results in formation of linear chains while the concentration of rings stays constant.[19] Thus, in effect, component buffering is caused by competition between ring formation by UPy-UPy association and end-capping by UPy-NaPy binding. This competition also explains why the onset of the buffering plateau - and concurrently UPy-NaPy binding - occurs at a much higher concentration than the binding of monotopic UPy and NaPy ($K_{UPy\text{-}NaPy} = 5 \times 10^6$ M^{-1}).[21] In other words, in region I the local concentration of UPy groups is simply too high to allow UPy-NaPy binding.

To verify whether the ring−chain supramolecular polymerization of ditopic UPy molecules **1a−c** can be described by a single effective molarity, concentration-dependent ^{1}H NMR measurements are performed. To this end, we probed the ^{1}H

DOI: 10.1021/ja5110377
J. Am. Chem. Soc. 2015, 137, 1501−1509

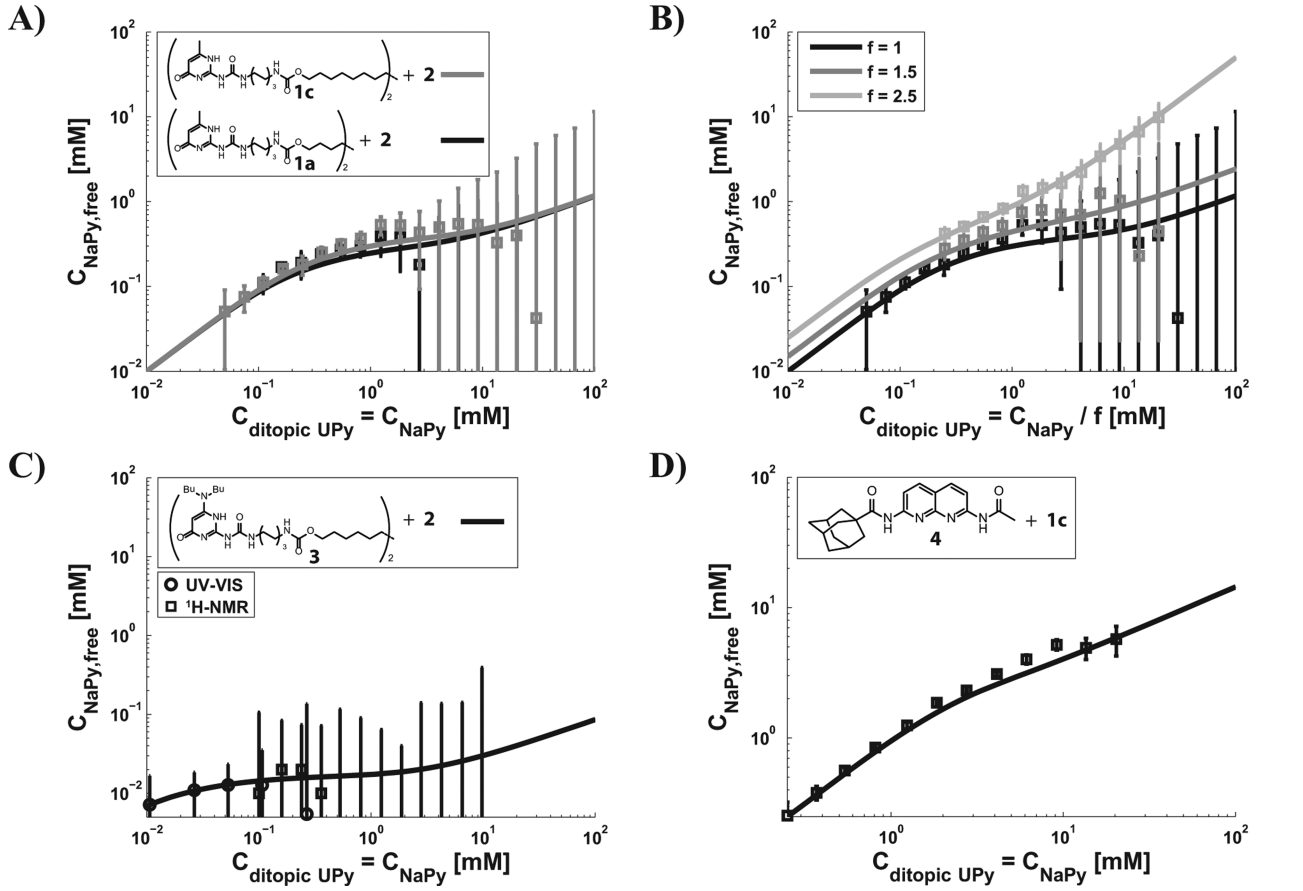

Figure 4. Free NaPy concentration versus total concentration for various experimental systems. (A) Mixtures of NaPy **2** with either ditopic UPy **1a** or **1c** (black and gray, respectively). (B) Mixtures of ditopic UPy **1c** and NaPy **2** at varying *f* ratios. (C) Mixtures of ditopic AminoUPy **3** and **2**. (D) Mixtures of adamantyl substituted NaPy **4** and ditopic UPy **1c**. The plots show experimental points based on ^{1}H NMR spectra (squares), UV−vis spectra (circles), and model predictions (lines). Error bars denote 95% confidence intervals based on assumed relative standard deviations of the mass, volume, and NMR integral (1, 1, and 5%, respectively). Note that in (D) most of the error bars are smaller than the marker size.

NMR signal of the urethane proton resulting in a concentration-dependent splitting that is assigned to either monomeric cycles, oligomeric cycles or linear chains (Figure 2; for assignment details, see the SI).[22] With the aggregation states assigned, the concentration-dependent fractions are analyzed using the ring−chain theory employing the reported value of $K_{UPy-UPy}$ in $CHCl_3$ ($K_{UPy-UPy} = 6 \times 10^7$ M^{-1}) as a fixed constant.[23] In the analysis, we performed nonlinear least-square analysis using two versions of the ring−chain equilibrium model, which vary in the number of effective molarities used during the fitting routine. In the first model, all cycles are considered strainless and thus a single effective molarity is used. In the second model, we employ two effective molarities, corresponding to the situation in which monomeric cycles behave as strained rings and dimeric and oligomeric rings are considered strainless.

In the assignment of the urethane peaks of ditopic UPy **1a**, it is not possible to distinguish chains and oligomeric cycles (Figure 2A). This indicates the similarity between the chemical environments of the urethane protons in both the oligomeric cycle and the chain conformation. The two models describe the experimental data of ditopic UPy **1a** equally well, suggesting that rings of ditopic UPy **1a** of any size are strainless.

Interestingly, for ditopic UPys **1b−c**, the second model considerably fits the data better than the first model (black versus gray solid lines in Figure 2B and C, respectively). Here it is observed that the optimized value of EM_1 as obtained by nonlinear least-square analysis is higher than expected based on eq 1 and the optimized value of the effective molarity of the strainless dimeric cycle, EM_2. This higher value of EM_1 with respect to EM_2 suggests that the monomeric ring is stabilized instead of being destabilized by ring strain. Indeed, this increase in stability is in line with a measured intramolecular hydrogen bond between the urethane proton and the carbonyl of the pyrimidinone in monomeric rings formed by **1b**.[22,24]

Although the model employing two EM values gives a slightly better description of the ring−chain competition of ditopic UPys **1b** and **1c**, the generality of supramolecular ring−chain buffering, which is based on the use of a single EM value, is not affected. Upon addition of NaPy, oligomeric rings are formed in very low amounts, which reduces the sensitivity of the buffering toward changes in EM_2 (for details, see the SI). Therefore, in the remainder of this work, we will demonstrate the principle of supramolecular ring−chain buffering by assuming that the ring−chain equilibrium of ditopic UPys can be described by a single EM value.

To evaluate the effect of changing the magnitude of EM_1 on the buffering behavior, several buffering curves were generated in which the EM_1 was varied and all other parameters are kept constant (Figure 3A). In line with the qualitative argument that buffering is predominantly caused by competition between ring formation and NaPy binding, both the buffering plateau

DOI: 10.1021/ja5110377
J. Am. Chem. Soc. 2015, 137, 1501−1509

concentration and broadness increase when increasing the EM_1; that is, the onset of the buffering plateau occurs at higher total concentrations since rings are more stable and $K_{UPy-NaPy}$ remains constant. Indeed, the opposite effect is observed when increasing the strength of UPy−NaPy binding by increasing $K_{UPy-NaPy}$ as the buffering onset occurs at lower total concentrations (Figure 3D). However, as a result of increasing $K_{UPy-NaPy}$ the $C_{NaPy-free}$ in region III also decreases, revealing the complexity of the supramolecular ring−chain buffering. The parameter $K_{UPy-UPy}$ also affects the onset of buffering, as it is not just the magnitude of the EM_1 that determines ring formation, but the product of EM_1 and $K_{UPy-UPy}$ (Figure 3C).[25] While varying the EM_1 does not change the $C_{NaPy-free}$ in region III, varying $K_{UPy-UPy}$ does, as the ratio of $K_{UPy-UPy}$ to $K_{UPy-NaPy}$ determines $C_{NaPy-free}$ when the system consists exclusively of chains. Varying the ratio of NaPy to ditopic UPy molecules (f) has the expected effect that the average $C_{NaPy-free}$ in the plateau decreases when decreasing f (Figure 3D). Interestingly, when f has a value around two, the slope of $C_{NaPy-free}$ in region III is extremely sensitive to small changes in f. When f is increased above two, the buffering completely vanishes due to the fact that the number of NaPy end-groups exceeds the number of UPy end-groups. This results in a system where end-capping is too dominant and only end-capped monomeric ditopic UPy molecules are present. Thus, only for f ratios below 2 buffering is observed over an appreciably wide concentration range.

2.2. Model Validation. The validity of the model describing supramolecular ring−chain buffering is confirmed by comparing model predicted buffering curves against ^{1}H NMR measurements using several different combinations of ditopic UPy and monotopic NaPy molecules (Figure 4). In effect, the molecules were chosen for their known variations in equilibrium binding constants or EMs, mostly only varying one parameter while others are kept constant. The equilibration time scale of freshly prepared or diluted mixtures was in the order of seconds, thus supramolecular buffering can be used for most, if not all, practical applications (see the SI). Since $C_{NaPy-free}$ cannot be measured directly using ^{1}H NMR, it is calculated by first determining the concentration of UPy groups in UPy−NaPy contacts ($C_{UPy-NaPy}$) via the following equation:

$$C_{UPy-NaPy} = 2C_{ditopic\text{-}UPy\text{-}total}\frac{I_{UPy-NaPy}}{I_{UPy-NaPy} + I_{UPy-UPy}} \quad (2)$$

where $I_{UPy-NaPy}$ and $I_{UPy-UPy}$ are the integrals of the signals corresponding to the N−H protons in the hydrogen bonding array of UPy−NaPy and UPy−UPy contacts, respectively. Subsequently, the free NaPy concentration is calculated via the mass balance of NaPy:

$$C_{NaPy-free} = C_{NaPy-total} - C_{UPy-NaPy} \quad (3)$$

where $C_{NaPy-total}$ is the total concentration of NaPy present in solution. This method of calculating $C_{NaPy-free}$ has the drawback of becoming increasingly uncertain when most of the NaPy molecules are bound. This uncertainty stems from the fact that as the fraction of free NaPy approaches zero, $C_{NaPy-total}$ and $C_{UPy-NaPy}$ approach values similar to each other. Small variations in the calculation of $C_{UPy-NaPy}$ due to experimental errors are then sufficient to create large uncertainties in $C_{NaPy-free}$. In our experiments, there are several sources of experimental error such as the uncertainty in determining the ^{1}H NMR integral and weighing and volumetric errors. To quantify the effect of those errors on the calculated $C_{NaPy-free}$, we employ relative standard deviations based on instrumental specifications and reported accuracies of NMR integrals.[26] As such, the plotted error bars are not based on multiple measurements of samples at the same total concentration, but are calculated based on a single measurement. The 95% confidence interval on $C_{NaPy-free}$ is calculated by standard error propagation techniques (see the SI).

Gratifyingly, all experimentally determined concentrations of free NaPy correspond well with model predictions based on reported binding constants and measured EMs. Interestingly, almost no difference in buffering is observed for ditopic UPy molecules **1a** and **1c** in mixtures with NaPy **2**. Even though their EMs differ by a factor of 2, the predicted buffering regime is almost overlapping. At high total concentrations, the experimental $C_{NaPy-free}$ values become negative and the error intervals become increasingly large due to the fact that the fraction of free NaPy becomes exceedingly small. Indeed, when the fraction of NaPy to ditopic UPy is increased to f = 2.5, and correspondingly the fraction of free NaPy does not approach zero at high concentrations, the uncertainty in $C_{NaPy-free}$ remains relatively small (Figure 4B). Contrary to our earlier report, the buffering curve is not measured at f = 2, since for this value the calculated concentrations of $C_{NaPy-free}$ are extremely sensitive to small errors (Figure 3B). Small amounts of impurities or weighing errors will then lead to vastly different buffering curves.

To verify the model prediction of changing the $K_{UPy-UPy}$, ditopic UPy **3** is synthesized following a modified literature procedure (for details of the synthesis, see the SI).[27a] The dibutyl amino group on ditopic UPy **3** stabilizes the enol as compared to the keto tautomer, resulting in a DADA hydrogen bonding array. Due to the negative secondary interactions of a DADA array as compared to the DDAA array of ditopic UPy **1**, the binding strength is a factor of 70 lower ($K_{UPy-UPy} = 9 \times 10^5$ M^{-1} in $CHCl_3$).[27] To obtain an EM_1 close to that of ditopic UPys **1a−c**, a dodecane linker is employed, as used in the synthesis of **1b**. The concentration-dependent ^{1}H NMR spectra show a splitting of the urethane proton resonance peak similar to the spectra of **1a−c** (see the SI). However, in contrast to said spectra, the relative intensities of the splitted peaks do not vary with increasing concentration. Instead, only a change in the chemical shift of one of the peaks is observed, from which C_{cr} is estimated to be 5 mM. This yields an EM_1 of 1.9 mM, which is reasonably similar to the EM_1 of ditopic UPy **1b** (9.0 ± 0.5 mM). Thus, with all input parameters of the model determined, the model prediction is verified by measuring $C_{NaPy-free}$ in mixtures of ditopic AminoUPy **3** and NaPy **2** (Figure 4C). Since the ^{1}H NMR measurements of these mixtures were prone to particularly large errors, additional measurements of $C_{NaPy-free}$ were performed using ultraviolet−visible (UV−vis) spectroscopy (for details, see the SI). Gratifyingly, the additional measurements overlap nicely with the model predictions.

Lastly, the model prediction obtained by varying $K_{UPy-NaPy}$ is verified by measuring mixtures of ditopic UPy **1c** and NaPy **4** that have a much lower binding constant due to steric hindrance of the adamantyl group.[28] As the heterocomplexation is less strong, the fraction of bound NaPy is lowered. Indeed, the model predicts the absence of buffering, in agreement with the experiments (Figure 4D). Decreasing $K_{UPy-NaPy}$ even further by increasing the steric hindrance, by use of a bis(adamantyl) substituted NaPy, resulted in the complete disappearance of the buffering regime (Figure S8).

DOI: 10.1021/ja5110377
J. Am. Chem. Soc. 2015, 137, 1501−1509

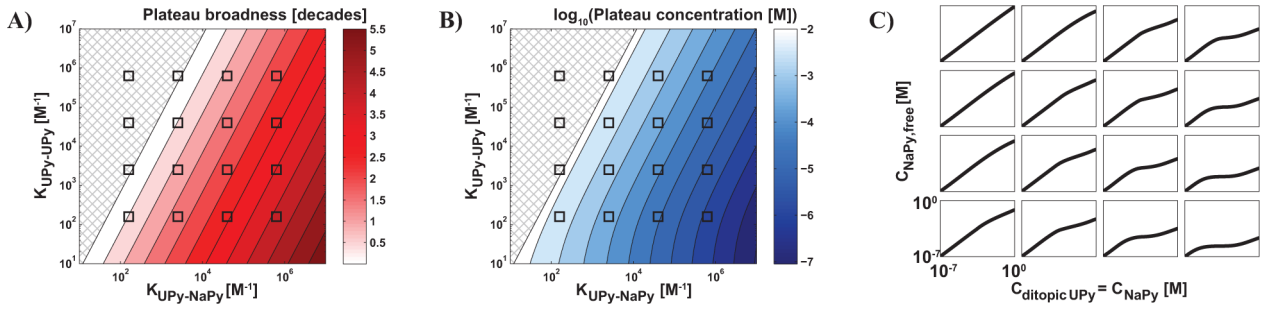

Figure 5. (A) Buffering plateau broadness and (B) the logarithm of the average plateau concentration as a function of $K_{UPy-UPy}$ and $K_{UPy-NaPy}$. EM_1 and f are fixed at 10 mM and 1, respectively. In the hatched region, no buffering is observed. The broadness is calculated analytically, while the plateau concentration is calculated numerically by taking the average of 10 logarithmically spaced points within the buffered range. Square markers denote the parameter values of the equilibrium binding constants that are used to generate the buffering curves in (C). All graphs of (C) have the same axis limits and scaling.

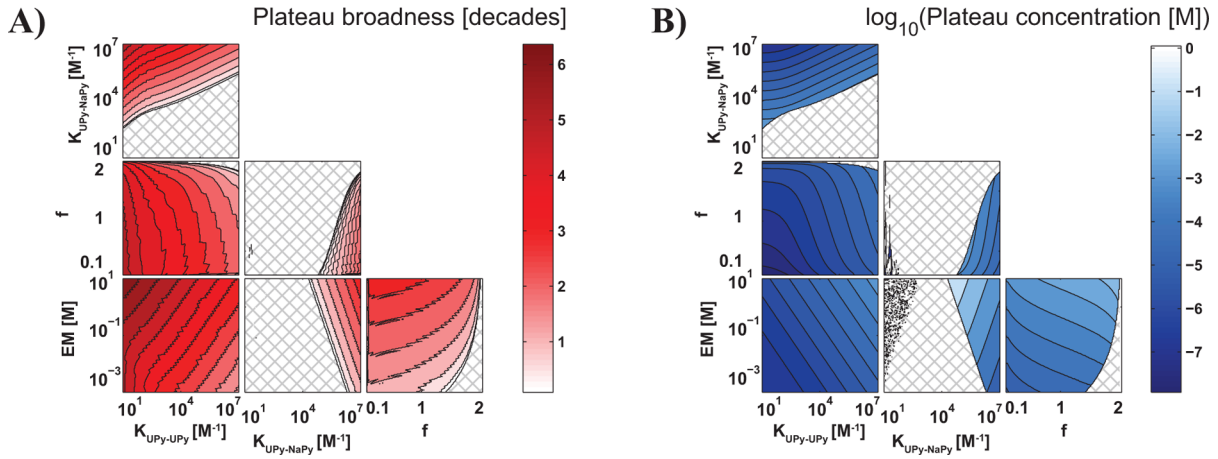

Figure 6. Multiparameter analysis of plateau broadness (A) and the logarithm of the plateau concentration (B) as a function of all model parameters. Parameters that are not varied are set to the following values: $K_{UPy-UPy} = 6 \times 10^7\ M^{-1}$, $K_{UPy-NaPy} = 5 \times 10^6\ M^{-1}$, $EM_1 = 0.01$ M, and $f = 1$. Hatched regions indicate that no buffering is observed. Both the plateau broadness and concentration are calculated numerically. The artifacts in the left half of the subplots in the second columns are due to numerical inaccuracies.

2.3. Design Principles of Supramolecular Ring−Chain Buffering. The experimental validation of the two component supramolecular ring−chain buffering model strongly suggests that it is applicable to a range of different ditopic molecules that can bind to a stopper molecule. Thus, as long as the binding constants and the EM values are known, the model can accurately predict the buffering behavior. This allows the rational design of molecular buffering systems, since the binding constants of many supramolecular associating groups are already reported.[29] While the EMs of smaller rings (<30 bonds) remain troublesome to predict, the order of magnitude of the EM for relatively large strainless rings (>30 bonds) can be accurately predicted.[20]

To derive the design principles of supramolecular ring−chain buffering, two quantities are evaluated: the broadness of the buffering plateau and the concentration of chain-stopper in the buffering regime (Figure 5). Interestingly, for the values of the binding constants used in Figure 5, a trade-off is observed between the plateau broadness and concentration: a high plateau concentration can only be achieved in conjunction with a low broadness and vice versa. Thus, it is clear that in order to obtain a specific buffering behavior, the ratio of homo- and heterodimerization is important, and not the absolute values. Intriguingly, this means that the model predicts that using a ditopic molecule with weakly associating end groups, such as benzoic acid, can give rise to a similar buffering plateau as one with strongly associating end groups such as ditopic UPy **1**.

It is hypothesized that the observed trade-off between the broadness of the buffering plateau and the concentration of free NaPy can be overcome. This is based on the observation that, for a single set of binding parameters, increasing the EM increases both the broadness and concentration simultaneously (Figure 3A). However, to verify that the EM can indeed overcome this trade-off, a way is required to report the influence of changing the EM while the other model parameters are varied across realistic values. We opted for performing a multiparameter analysis in which every combination of two parameters is varied while the other two are kept at a constant value. Comparing the graphs in which the EM is varied, it is observed that increasing the EM indeed increases both the plateau broadness and concentration for all of the parameter values considered here (Figure 6, bottom graphs). This strongly suggests that increasing the EM has the same effect of overcoming the trade-off for all combinations of the other parameters.

In the optimization of the supramolecular ring−chain buffering, it becomes readily apparent that there are no clear requirements for an optimal type of buffer. Instead, optimality depends strongly on the desired buffer properties for a specific

DOI: 10.1021/ja5110377
J. Am. Chem. Soc. 2015, 137, 1501−1509

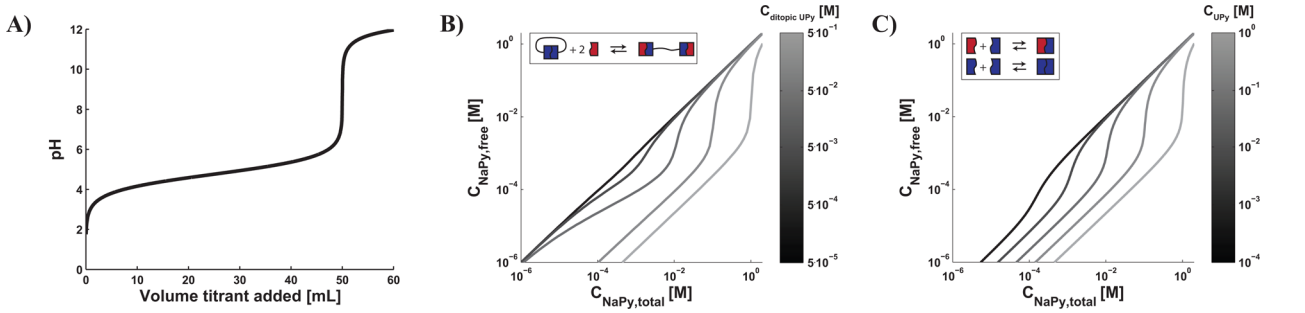

Figure 7. (A) Simulated titration curve of an acidified solution of a weak acid (pK_a = 4.7, 0.1 M, 50 mL) with a strong base (0.1 M). (B) Simulated supramolecular ring−chain buffering curves describing the addition of NaPy to a solution containing fixed concentrations of ditopic UPy. $K_{UPy-UPy}$ = 6×10^7 M^{-1}, $K_{UPy-NaPy}$ = 5×10^6 M^{-1}, and EM_1 = 10 mM. (C) Simulated molecular titration curves describing the addition of NaPy to a solution containing fixed concentrations of monotopic UPy. $K_{UPy-UPy}$ = 6×10^7 M^{-1} and $K_{UPy-NaPy}$ = 5×10^6 M^{-1}.

application. Thus, two example cases are considered here in terms of their required parameters.

(I) Biological reporter molecules are usually present in low concentrations (nM regime) and can be buffered across a wide range of total concentrations. Thus, a buffer with a high broadness and low concentration is applicable, which requires, for example, a construct of two associating proteins linked by a flexible chain.[18,30] Peptide chains can be designed to be flexible random coil chains, which are accurately described using the wormlike chain or Gaussian chain model, which gives a high degree of control over the EM.[31] Because the buffering is to take place at low concentrations, the EM of the ditopic construct can be relatively low (μM to mM regime). The appropriate binding strengths of the ditopic and monotopic molecules can then be chosen by generating a graph similar to Figure 5. Using Figure 5 as an example, the binding constants should be chosen to be in the right-lower region of the graph to obtain a buffer with a broad plateau and low concentration.

(II) Chemical catalysts are mostly used at higher concentrations (mM to M regime) while their operating concentrations are limited to a relatively small range. Therefore, a buffer with high concentration and low broadness is best suited. The combination of supramolecular interactions and catalysis is well explored; thus, it should pose no challenge designing ditopic molecules with binding groups that can deactivate a catalyst when bound to the catalyst.[32] Since the buffering plateau is limited at high concentration by the critical concentration and since the magnitude of the critical concentration is a direct result of the magnitude of the EM, the EM should at least be equally high as the desired operating concentration. This imposes some strict design rules on the linker, as obtaining a high EM is not always straightforward.[33] This stems from the fact that short linkers are conformationally more limited and give rise to odd−even effects in the EM with respect to the linker length.[20] The requirements on the binding constants are less strict, and can again be chosen by generating a graph similar to Figure 5.

2.4. Buffering by a Ring−Chain Mechanism versus Other Buffering Mechanisms. The principle of supramolecular ring−chain buffering as demonstrated in the previous sections, where buffering is observed while the total concentrations of *both* components are changed, is dissimilar from "traditional" pH buffering in the sense that one generally does not change the total concentrations of both the buffering and the buffered molecules in a pH buffer. Instead, in a pH buffer, the concentration of the buffered molecule (protons) is made insensitive to addition of acids or bases by action of a weak acid that acts as the buffering agent (Figure 7A). Thus, the question is raised whether the free NaPy concentration is buffered when NaPy is added to a solution containing a fixed concentration of ditopic UPy.

Based on the observation that supramolecular ring−chain buffering is caused by competition between the formation of cycles and end-capped chains, it is expected that the initial concentration of ditopic UPy plays a crucial role in buffering. Indeed, the supramolecular ring−chain buffering curves generated by employing ditopic UPy concentrations below the critical concentration have slopes smaller than unity, reminiscent of pH titration curves (Figure 7B). While the slopes of supramolecular buffering curves are not as low as those of pH titration curves (indicating room for improvement), this does present the first example of supramolecular buffering. In contrast to pH buffers, the scope of our system is much broader as it enables buffering of a wide range of molecules with, for example, various catalytic functions. Concomitant to pH buffering, an increase in the initial ditopic UPy concentration, up to the critical concentration, leads to an increase in the buffer capacity.[34]

Increasing the initial ditopic UPy concentration above the critical concentration leads to ultrasensitive threshold behavior. Ultrasensitive threshold behavior can be generated by various molecular mechanisms, such as positive feedback or molecular titration.[35] In the latter case, active components are stoichiometrically sequestered by reversible binding to strong inhibitors up until the equivalence point set by the concentration of the inhibitor.[12c,36] Once the inhibitor sink is filled, an increase in the total concentration of active component then results in a steep increase in the concentration of free active monomer (Figure 7C). The molecular titration curves overlap with the curves of supramolecular ring−chain buffering that have a ditopic UPy concentration above the critical concentration ($C_{monotopic\text{-}UPy} = 2C_{ditopic\text{-}UPy}$), indicating that ring formation is negligible at high ditopic UPy concentrations. Thus, supramolecular buffering by ring−chain equilibria extends the ultrasensitivity of molecular titration to include buffering, or subsensitivity, at concentrations below the threshold, allowing for extended regulatory capabilities. The ubiquitous presence of ditopic, tritopic, and multitopic proteins in biochemical pathways suggests that supramolecular ring−chain buffering in biological networks is yet to be discovered.[30b]

3. CONCLUSIONS

We report a method to expand the scope of buffering from exclusively protons to whole molecules that are equipped with

DOI: 10.1021/ja5110377
J. Am. Chem. Soc. 2015, 137, 1501−1509

supramolecular binding groups. This is achieved by a ditopic molecule that is able to form rings and chains, and which is functionalized with binding groups complementary to the buffered monotopic molecule. By studying a newly developed thermodynamic equilibrium model of buffering, we were able to deduce that buffering occurs by competition between ring formation and stopper binding. The influence of the key model parameters was determined and the model was validated using a library of buffering systems, each with varying physicochemical parameters. The design principles of supramolecular ring−chain buffering are elucidated by further model evaluation, revealing that the EM is the critical model parameter in attaining a buffering plateau with both a high broadness and a high concentration. We expect that this is the first step in broadening the definition of buffering as currently used in chemistry. The present system might be further expanded to include A−B type ditopic molecules or ternary systems that can be employed to generate more diverse behavior.[37] Future work will focus on creating a chemical buffering system with feedback loops to mimic Nature's way of component buffering more accurately.

■ ASSOCIATED CONTENT

Supporting Information

Detailed experimental procedures, complete characterization of compounds, supramolecular buffering model derivation, ring−chain analysis of ditopic UPys, confidence interval calculations, buffering curve of bis(adamantyl) NaPy **8**-ditopic UPy **1c** mixtures, UV−vis data of ditopic UPy **3**−NaPy **2** mixtures, and kinetic ^{1}H NMR data. This material is available free of charge via the Internet at http://pubs.acs.org.

■ AUTHOR INFORMATION

Corresponding Authors

t.f.a.d.greef@tue.nl
e.w.meijer@tue.nl

Notes

The authors declare no competing financial interest.

■ ACKNOWLEDGMENTS

The authors would like to thank Anja Palmans for stimulating discussions and valuable feedback on the manuscript. The authors would also like to thank Francisco Rodriguez-Llansola, Bram Teunissen, and Marko Nieuwenhuizen for stimulating discussions and generously providing synthetic compounds. This work is financed by The Netherlands Organisation for Scientific Research (NWO VENI Grant: 722.012.0001 and NWO Graduate Programme 2010:022.002.028), the Dutch Ministry of Education, Culture and Science (Gravity program 024.001.035), and the European Research Council (FP7/2007-2013, ERC Advanced Grant No. 246829).

■ REFERENCES

(1) (a) Stuart, M. A. C.; Huck, W. T. S.; Genzer, J.; Müller, M.; Ober, C.; Stamm, M.; Sukhorukov, G. B.; Szleifer, I.; Tsukruk, V. V.; Urban, M.; Winnik, F.; Zauscher, S.; Luzinov, I.; Minko, S. *Nat. Mater.* **2010**, *9*, 101. (b) De las Heras Alarcón, C.; Pennadam, S.; Alexander, C. *Chem. Soc. Rev.* **2005**, *34*, 276. (c) Rybtchinski, B. *ACS Nano* **2011**, *5*, 6791.

(2) (a) Giuseppone, N.; Lehn, J.-M. *J. Am. Chem. Soc.* **2004**, *126*, 11448. (b) Moulin, E.; Cormos, G.; Giuseppone, N. *Chem. Soc. Rev.* **2012**, *41*, 1031. (c) Busseron, E.; Ruff, Y.; Moulin, E.; Giuseppone, N. *Nanoscale* **2013**, *5*, 7098. (d) Ikeda, M.; Tanida, T.; Yoshii, T.; Kurotani, K.; Onogi, S.; Urayama, K.; Hamachi, I. *Nat. Chem.* **2014**, *6*, 511. (e) Nguyen, R.; Jouault, N.; Zanirati, S.; Rawiso, M.; Allouche, L.; Fuks, G.; Buhler, E.; Giuseppone, N. *Soft Matter* **2014**, *10*, 3926.

(3) Lehn, J.-M. *Angew. Chem., Int. Ed.* **2013**, *52*, 2836.

(4) (a) Lee, D. H.; Severin, K.; Ghadiri, M. R. *Curr. Opin. Chem. Biol.* **1997**, *1*, 491. (b) Rowan, S. J.; Cantrill, S. J.; Cousins, G. R. L.; Sanders, J. K. M.; Stoddart, J. F. *Angew. Chem., Int. Ed.* **2002**, *41*, 898. (c) Vidonne, A.; Philp, D. *Eur. J. Org. Chem.* **2009**, 593. (d) Giuseppone, N. *Acc. Chem. Res.* **2012**, *45*, 2178. (e) Li, J.; Nowak, P.; Otto, S. *J. Am. Chem. Soc.* **2013**, *135*, 9222. (f) Ludlow, R. F.; Otto, S. *Chem. Soc. Rev.* **2008**, *37*, 101.

(5) (a) Ross, J.; Arkin, A. P. *Proc. Natl. Acad. Sci. U. S. A.* **2009**, *106*, 6433. (b) Lehn, J.-M. In *Constitutional Dynamic Chemistry*; Barboiu, M., Ed.; Springer: Berlin, Heidelberg, 2011; Vol. *322*, pp 1−32.

(6) Saggiomo, V.; Hristova, Y. R.; Ludlow, R. F.; Otto, S. *J. Syst. Chem.* **2013**, *4*, 1.

(7) (a) Tjivikua, T.; Ballester, P.; Rebek, J., Jr. *J. Am. Chem. Soc.* **1990**, *112*, 1249. (b) Von Kiedrowski, G. In *Bioorganic Chemistry Frontiers*; Springer: Berlin Heidelberg, 1993; Vol. 3, pp 113−146. (c) Dadon, Z.; Wagner, N.; Ashkenasy, G. *Angew. Chem., Int. Ed.* **2008**, *47*, 6128. (d) Wagner, N.; Ashkenasy, G. *J. Chem. Phys.* **2009**, *130*, 164907. (e) Moulin, E.; Giuseppone, N. In *Constitutional Dynamic Chemistry*; Barboiu, M., Ed.; Springer: Berlin Heidelberg, Berlin, Heidelberg, 2011; Vol. *322*, pp 87−105.

(8) Carnall, J. M. A.; Waudby, C. A.; Belenguer, A. M.; Stuart, M. C. A.; Peyralans, J. J.-P.; Otto, S. *Science* **2010**, *327*, 1502.

(9) (a) Allen, V. C.; Robertson, C. C.; Turega, S. M.; Philp, D. *Org. Lett.* **2010**, *12*, 1920. (b) Wagner, N.; Ashkenasy, G. *Chem. - Eur. J.* **2009**, *15*, 1765.

(10) (a) Perrin, D. D.; Dempsey, B. In *Buffers for pH and Metal Ion Control*; Springer: New York, 1974. (b) Cross, J. S.; Clausen, E. C. *Biomass Bioenergy* **1993**, *4*, 277. (c) Youssef, Y. A.; Ahmed, N. S. E.; Mousa, A. A.; El-Shishtawy, R. M. *J. Appl. Polym. Sci.* **2008**, *108*, 342.

(11) Oxtoby, D. W.; Gillis, H. P.; Nachtrieb, N. H. *Principles of modern chemistry*; Thomson/Brooks/Cole: Belmont, CA, 2002.

(12) (a) Becskei, A.; Serrano, L. *Nature* **2000**, *405*, 590. (b) Whitaker, W. R.; Davis, S. A.; Arkin, A. P.; Dueber, J. E. *Proc. Natl. Acad. Sci. U. S. A.* **2012**, *109*, 18090. (c) Buchler, N. E.; Louis, M. *J. Mol. Biol.* **2008**, *384*, 1106.

(13) De Greef, T. F. A.; Smulders, M. M. J.; Wolffs, M.; Schenning, A. P. H. J.; Sijbesma, R. P.; Meijer, E. W. *Chem. Rev.* **2009**, *109*, 5687.

(14) (a) Guler, M. O.; Stupp, S. I. *J. Am. Chem. Soc.* **2007**, *129*, 12082. (b) Rodríguez-Llansola, F.; Escuder, B.; Miravet, J. F. *J. Am. Chem. Soc.* **2009**, *131*, 11478. (c) Cantekin, S.; ten Eikelder, H. M. M.; Markvoort, A. J.; Veld, M. A. J.; Korevaar, P. A.; Green, M. M.; Palmans, A. R. A.; Meijer, E. W. *Angew. Chem., Int. Ed.* **2012**, *51*, 6426.

(15) Rodríguez-Llansola, F.; Meijer, E. W. *J. Am. Chem. Soc.* **2013**, *135*, 6549.

(16) Teunissen, A. J. P.; van der Haas, R. J. C.; Vekemans, J. A. J. M.; Palmans, A. R. A.; Meijer, E. W. Manuscript in preparation.

(17) Jacobson, H.; Stockmayer, W. H. *J. Chem. Phys.* **1950**, *18*, 1600.

(18) Bastings, M. M. C.; de Greef, T. F. A.; van Dongen, J. L. J.; Merkx, M.; Meijer, E. W. *Chem. Sci.* **2010**, *1*, 79.

(19) Ercolani, G.; Mandolini, L.; Mencarelli, P.; Roelens, S. *J. Am. Chem. Soc.* **1993**, *115*, 3901.

(20) Mandolini, L. In *Advances in Physical Organic Chemistry*; Gold, V., Bethell, D., Eds.; Academic Press: London, 1987; Vol. *22*, pp 1−111.

(21) Ligthart, G. B. W. L.; Ohkawa, H.; Sijbesma, R. P.; Meijer, E. W. *J. Am. Chem. Soc.* **2005**, *127*, 810.

(22) Teunissen, A. J. P.; Nieuwenhuizen, M. M. L.; Rodríguez-Llansola, F.; Palmans, A. R. A.; Meijer, E. W. *Macromolecules* **2014**, *47*, 8429−8436.

(23) Söntjens, S. H. M.; Sijbesma, R. P.; van Genderen, M. H. P.; Meijer, E. W. *J. Am. Chem. Soc.* **2000**, *122*, 7487.

(24) Lafitte, V. G. H.; Aliev, A. E.; Horton, P. N.; Hursthouse, M. B.; Hailes, H. C. *Chem. Commun.* **2006**, 2173.

DOI: 10.1021/ja5110377
J. Am. Chem. Soc. 2015, 137, 1501−1509

(25) (a) Hunter, C. A.; Anderson, H. L. *Angew. Chem., Int. Ed.* **2009**, *48*, 7488. (b) Ercolani, G.; Schiaffino, L. *Angew. Chem., Int. Ed.* **2011**, *50*, 1762.
(26) Bain, A. D.; Fahie, B. J.; Kozluk, T.; Leigh, W. J. *Can. J. Chem.* **1991**, *69*, 1189.
(27) (a) Felder, T.; de Greef, T. F. A.; Nieuwenhuizen, M. M. L.; Sijbesma, R. P. *Chem. Commun.* **2014**, *50*, 2455. (b) Jorgensen, W. L.; Pranata, J. *J. Am. Chem. Soc.* **1990**, *112*, 2008. (c) Pranata, J.; Wierschke, S. G.; Jorgensen, W. L. *J. Am. Chem. Soc.* **1991**, *113*, 2810. (d) Quinn, J. R.; Zimmerman, S. C.; Del Bene, J. E.; Shavitt, I. *J. Am. Chem. Soc.* **2007**, *129*, 934.
(28) Ligthart, G. B. W. L. Complementary quadruple hydrogen bonding. Ph.D. Thesis, Eindhoven University of Technology, Eindhoven, 2006.
(29) (a) Zimmerman, S. C.; Corbin, P. S. In *Molecular Self-Assembly Organic Versus Inorganic Approaches*; Fuiita, M., Ed.; Springer: Berlin, Heidelberg, 2000; pp 63−94. (b) Wilson, A. J. *Soft Matter* **2007**, *3*, 409.
(30) (a) Fegan, A.; White, B.; Carlson, J. C. T.; Wagner, C. R. *Chem. Rev.* **2010**, *110*, 3315. (b) Hobert, E. M.; Doerner, A. E.; Walker, A. S.; Schepartz, A. *Isr. J. Chem.* **2013**, *53*, 567.
(31) Evers, T. H.; van Dongen, E. M. W. M.; Faesen, A. C.; Meijer, E. W.; Merkx, M. *Biochemistry* **2006**, *45*, 13183.
(32) (a) Wilkinson, M. J.; Leeuwen, P. W. N. M.; van Reek, J. N. H. *Org. Biomol. Chem.* **2005**, *3*, 2371. (b) Dydio, P.; Breuil, P.-A. R.; Reek, J. N. H. *Isr. J. Chem.* **2013**, *53*, 61. (c) Gianneschi, N. C.; Cho, S.-H.; Nguyen, S. T.; Mirkin, C. A. *Angew. Chem.* **2004**, *116*, 5619. (d) Yoon, H. J.; Kuwabara, J.; Kim, J.-H.; Mirkin, C. A. *Science* **2010**, *330*, 66. (e) Wiester, M. J.; Ulmann, P. A.; Mirkin, C. A. *Angew. Chem., Int. Ed.* **2011**, *50*, 114.
(33) (a) Adams, H.; Chekmeneva, E.; Hunter, C. A.; Misuraca, M. C.; Navarro, C.; Turega, S. M. *J. Am. Chem. Soc.* **2013**, *135*, 1853. (b) Sun, H.; Hunter, C. A.; Navarro, C.; Turega, S. *J. Am. Chem. Soc.* **2013**, *135*, 13129.
(34) Skoog, D. A.; West, D. M.; Holler, F. J.; Crouch, S. R. *Fundamentals of Analytical Chemistry*, 8th ed.; Cengage: Belmont, CA, 2004.
(35) Zhang, Q.; Bhattacharya, S.; Andersen, M. E. *Open Biol.* **2013**, *3*, 130031.
(36) (a) Mukherji, S.; Ebert, M. S.; Zheng, G. X. Y.; Tsang, J. S.; Sharp, P. A.; van Oudenaarden, A. *Nat. Genet.* **2011**, *43*, 854. (b) Semenov, S. N.; Markvoort, A. J.; Gevers, W. B. L.; Piruska, A.; de Greef, T. F. A.; Huck, W. T. S. *Biophys. J.* **2013**, *105*, 1057.
(37) Douglass, E. F.; Miller, C. J.; Sparer, G.; Shapiro, H.; Spiegel, D. A. *J. Am. Chem. Soc.* **2013**, *135*, 6092.

DOI: 10.1021/ja5110377
J. Am. Chem. Soc. 2015, 137, 1501−1509